

Improved corrosion resistance in biomaterial applications of the AISI 316L alloy

Saja A. Abdul Maged¹, Rusul Salah Hadi^{1*} 

¹ University of Technology, Baghdad, Iraq

* Corresponding author's e-mail: rusul.s.hadi@uotechnology.edu.iq

ABSTRACT

This paper addresses the corrosion performance of the AISI 316L stainless steel, an important biomaterial, in simulated physiological environments and aggressive media. Rectangular samples (1 × 1 cm, 1 mm thickness) were prepared from 316L alloy and electrochemical tests were performed in a 3 electrode cell at 37 °C ± 0.4 °C. Potentiodynamic polarization curves were recorded after 2 hours of immersion in Ringer's solution and other media with an overvoltage range of [-400 mV, +400 mV] versus Ag/AgCl. The polarization resistance in Ringer's solution was 2.1 kΩ·cm² (±0.18) with corrosion current density of 0.23 μA/cm², which was better than the NaCl and HNO₃ solutions. The carbonate ions in Ringer's inhibited the pitting corrosion pathway while low carbon content in the alloy prevented the formation of carbides at grain boundaries inhibiting intergranular corrosion. These results demonstrate that the homogeneity of the alloy and stability of the passive film are both essential to corrosion resistance and influenced by other factors, such as chemical composition, structure, and environmental condition. These findings provide evidence for the AISI 316L stainless steel as appropriate biomedical material where long-term corrosion resistance is an important design factor.

Keywords: corrosion resistance, AISI 316L stainless steel, ringer solution, electrochemical testing, passive film stability.

INTRODUCTION

Biomaterials are considered a major therapeutic revolution of the late 20th century. Initially reserved for critical situations, they are now used to meet patients' needs in rehabilitation, comfort, pleasure, and aesthetics. [1] A biomaterial is defined as a non-living material designed to interact with biological arrangements. Biomaterials are primarily used in orthopedics (hip, elbow, knee, and wrist prostheses, orthoses, artificial ligaments, and tendons), dentistry (restoration materials, dental and bone fillers, and implants), ophthalmology (lenses and implants), as well as cardiovascular systems (heart valves, artificial hearts, and pacemakers) [2]. Unfortunately, metallic materials used as implants are susceptible to corrosion in body fluids, despite their high corrosion resistance. The corrosion products released

by the material diffuse into tissues, causing toxic effects and health degradation of the host [3, 4].

“Biomaterials” refer to any material used in medical implants, extracorporeal devices as well as instruments in medicine, hospital, dentistry, and veterinary medicine. The National Institutes of Health Consensus Development Conference (1991) defined a biomaterial as “any material intended to interface with living tissues and/or biological fluids to evaluate, treat, augment, or replace any tissue, organ, or function of the body”. They differ from drugs in that they do not achieve their primary therapeutic purpose through a chemical effect within the body and do not need to be metabolized to be active. The public denominator in all definitions planned for biomaterials is the clear recognition that biomaterials are distinct from additional classes of materials due to the special biocompatibility criteria they must meet [3].

Biomaterials are considered a major therapeutic revolution of the late 20th century. Initially reserved for critical situations, they are now used to meet patients' needs in rehabilitation, comfort, pleasure, and aesthetics [1]. A biomaterial is defined as a non-living material designed to interact with biological arrangements. Biomaterials are primarily used in orthopedics (hip, elbow, knee, and wrist prostheses, orthoses, artificial ligaments, and tendons), dentistry (restoration materials, dental and bone fillers, and implants), ophthalmology (lenses and implants), as well as cardiovascular systems (heart valves, artificial hearts, and pacemakers) [2]. Unfortunately, metallic materials used as implants are susceptible to corrosion in body fluids, despite their high corrosion resistance. The corrosion products released by the material diffuse into tissues, causing toxic effects and health degradation of the host [3, 4].

For an implantation to be a success, the biomaterial used must, on the one hand, meet the physicochemical characteristics appropriate to the installation site and the function to be fulfilled and on the other hand, it must be compatible [5].

The biological study of biomaterials consists, firstly, in the study of the recipient site on the physical, chemical and biological levels in static and dynamic situations. This is followed by a study of the biocompatibility and bio-functionality of biomaterials, in order to deduce the interactions that may exist between implants and tissues and/or organic fluids, under normal or pathological conditions [6, 7].

Water represents 45 to 75% of the body weight. It is divided into an intracellular sector (69.8%) and another extracellular sector which is represented by plasma (8.2%) and the ground substance (22%). The biological environment is essentially represented on the ionic level by sodium ions (Na^+ , 140 mEq/L) and chloride (Cl^- , 100 mEq/L), i.e. a concentration of 9 g/l of NaCl. There are 6 mEq/L of organic acids with a pH of 7.4. The partial pressure of oxygen is 90 mm of mercury and that of carbon dioxide is 40 mm of mercury. It is also necessary to be aware of the complexity of cellular enzymatic phenomena involving oxidation, reduction, hydrolysis processes and the importance of metal ions during enzymatic reactions. Inflammation, necrosis, or infection will modify or disrupt these reaction chains, cause them to take anaerobic paths and possibly modify the pH [8]. Similar polarization resistance trends in simulated physiological environments have been demonstrated recently in

IOP Conference Series: Materials Science and Engineering [9].

On a molecular scale, the human body is constantly evolving. The presence of enzymes (proteins) in the body plays a role of catalyst which influences the speed of biochemical reactions between the different constituent elements (water, ionic group, organic acids, etc.) [8, 10].

The effect of pH is sensitive. An alkaline solution up to pH 12 protects metals from corrosion. An acidic pH acts on the oxide layer covering the metal. This action creates a departure of oxides, which exposes the underlying metal. The metal thus uncovered is in turn subject to oxidation. This phenomenon initiates the phenomenon of corrosion [10, 11].

According to some authors, the anions and cations formed by hydrolysis under the effect of corrosion mean that in the tissue (electrolyte), an exchange of proton H^+ occurs, thus causing the change in pH, hence the denaturation of the organic matter [12, 13].

The physical characterization of the recipient site is particularly important for implants with a functional substitution role. The components of the site concerned must be studied first in statics, by analyzing its composition, its spatial, cellular, tissue and anatomical organization. The physical study must also take into account the evolutionary nature of the system considered. It is advantageous to use an implant made of a material the mechanical performance of which is not affected by pH variations.

It is essential to know certain mechanical characteristics, such as: tensile strength, compression, torsion, bending, modulus of elasticity, elastic limit, fatigue resistance, hardness, coefficient of friction, distribution, direction, importance of the forces exerted, etc. All these elements are not always known with extreme precision and the refinement of knowledge in biomechanics should generate particularly remarkable advances. However, wanting to substitute biomaterials in a stable way for tissues with remarkable short- and long-term adaptation capacities will remain a very difficult challenge for a long time to come [1, 14].

Corrosion resistance, chemical inertness with respect to the environment (in particular the salivary environment for dental implants) and biocompatibility are the properties that must be controlled to maintain the integrity of the material. For dental implants, the conditions are even more severe, since the salivary environment contains

more sulfur products that make it more corrosive. All these points must be respected, otherwise the prosthesis will have to be replaced often or the reactions that endanger the patient's health will be observed [15, 16].

Metals have been used as biomaterials for centuries, a wrought iron dental implant was discovered on a young man who lived in Gallo-Roman times, but it was only with the advent of asepsis that they entered surgical practice. Nowadays, metallic biomaterials are mainly used in orthopedics (screws, nails, joints, plates, etc.), in stomatology (fillings, prostheses, denture parts, etc.) and in surgery (tools). Metals and alloys are used as biomaterials in the applications where their properties are particularly suited to the requirements of the function to be fulfilled. There is a wide variety of metallic materials used as biomaterials, some of which are presented in Table 1 [17, 18].

Metals are materials that generally crystallize in a hexagonal close-packed (HC) or face-centered cubic (FCC) structure. Metallic crystals have specific properties defined using parameters, depending on the strength, ductility, conductivity, etc. These properties are related to the number and type of imperfections. Meyrueis and Gotman summarize the characteristics and properties that metals or their alloys must have in order to meet the criteria of biocompatibility, corrosion resistance, and sufficient mechanical qualities to replace failing organs. Many pure metals

have been used by surgeons, but their properties were sometimes insufficient: iron is not very resistant to corrosion, lead is toxic, copper is not very biocompatible and not very mechanically resistant like platinum or gold. As a result, titanium is the most widely used pure metal. Today, three major families of alloys emerge and meet the criteria mentioned above: SS, cobalt-based alloys and titanium-based alloys. Since the human body is a corrosive environment, the alloys used must have a regenerative passivation layer, the combination of two types of alloys to produce a prosthetic device must consider galvanic corrosion. Rigidity (property to oppose deformation) and flexibility (easy deformation of the metal) complete the selection criteria. The work hardening of a metal, deformation in its plastic zone by forging, by drawing, by cold rolling modifies the mechanical properties. Reheating or annealing in a certain temperature range restores some of the desired initial qualities. The fatigue limit, also called endurance limit, often corresponds to 50% of the breaking load. The production of joint prostheses requires implants with a high breaking load because the stresses they support are considerable. The high rigidity of cobalt-chromium alloys and SS does not propagate a large part of the stresses exerted by the bone [19, 20]. Table 2 presents some mechanical and technical characteristics of metals and alloys used for the production of surgical implants [19, 21].

Table 1. Main metal alloys used as biomaterials and their uses

Base elements	Main alloying elements	Generic name	Typical applications
Iron	C, Cr, Ni, Mn, Mo, V	SS (stainless steels)	Osteosynthesis materials, surgical instruments
Cobalt	Cr, Mn, Mo, Ni, Nb, Ta	Chrome-based alloys	Articular prosthesis components
Titanium	Al, V, Fe, Nb, Zr	Titanium-based alloys	Osteosynthesis materials, articular prosthesis components, surgical instruments
Platinum	Ir, Pb	Precious alloys	Electrodes

Table 2. Mechanical and technical characteristics of metals and alloys used for the production of surgical implants

Material	Elemental composition (%)	Elastic modulus (GPa)	Yield strength (MPa)	Elongation (%)	Surface
Ti	99	97–116	240–550	> 15	Ti Oxide
Ti-Al-V	Ti-6Al-4V	117–130	860–898	> 12	Ti Oxide
Co-Cr-Mo	66Co-27Cr-7Mo	235	655	> 08	Cr Oxide
316L	70Fe-18Cr-12Ni	193	480–1000	> 30	Cr Oxide
Ta	99	150–186	690	11	Ta Oxide
Au	99	97	–	> 30	Au
Pt	99	207–310	131	40	Pt

Of all the types of SS, austenitic ones have the best corrosion resistance; they contain both Chromium and Nickel as well as have an austenitic crystal structure [22]. The specifications for surgical austenitic SS, usually called 316L, are typically 17–20% Chromium, 12–14% Nickel and 1.2–4% Molybdenum with a maximum of 0.03% Carbon. They have high hardness and toughness. Although they contain Chromium, their corrosion resistance is not very good, as a result a breakdown of the passivation film leading to significant corrosion is observed. This can compromise biocompatibility and also release corrosion products that have harmful effects on tissues [23, 24]. In order to improve corrosion resistance, solid solutions in stable austenite (Ni > 12 to 14) are used. A molybdenum concentration greater than 2% ensures a higher resistance to perforating corrosion while a low carbon content that is less than or equal to 0.03% inhibits the formation of carbides and deformation martensite. In addition, for surgical tools such as scalpels, needles or scissors, chromium steels are often used which support higher stresses [23]. Other modifications can be made to the steel to improve these mechanical properties: increasing the chromium, molybdenum and nickel content makes the material non-magnetic; reducing the manganese, sulfur and aluminum content removes inclusions (MnS) and thus improves the resistance to fatigue and localized corrosion (pitting); reducing the carbon content prevents intergranular corrosion. One can also intervene on the production method (in particular by using vacuum remelting, which improves cleanliness with respect to oxides) and at the level of the method of transformation by hyperquenching of the material (which prevents intergranular corrosion and fatigue failure) or by homogeneous work hardening and forging (which increases the mechanical characteristics, avoiding reducing the resistance to corrosion linked to heterogeneous work hardening), finally the manufacturer can intervene on the surface condition to prevent any cracking, pitting, etc. The implants made of SS are used as temporary implants to service bone healing, as well as fixed implants such as artificial links. Typical temporary requests are plates, medullary nails, screws and pins [25, 26].

In recent years, advances in materials science have illuminated the properties of underlying factors affecting the corrosion resistance properties of SS used in biomedical products. For example, low alloy steels have shown that mechanical

properties are crucial to the overall performance of materials with consideration to the efficacy and durability of biomedical components [27]. Stainless welding has also demonstrated the effect of surface treatments or sample preparation on corrosive behavior and this reinforces that controlled, reproducible condition needs to be carried out experimentally [28]. The same emphasis on degradation of composite materials has found strong correlations between degradation processes on both compositional and surface properties with similar degradation / corrosion identified in the outcomes of the SEM analysis [29]. Different methodological approaches resulting from analyses and thermal conditions could be beneficial in informing potential experimental testing for a well-rounded evaluation of material behaviors under physiological and environmental conditions [30]. Newly published works on different environments affecting the material performance can also serve as pointers for interpreting the results of electrochemical and surface analyses as it relates to simulating key conditions in corrosion studies [31]. Overall, contemporary studies will help elucidate the understanding of corrosion resistance properties of the AISI 316L stainless steel.

The conducted study focused on the corrosion of one material used as implants: austenitic SS 316L. [32, 33] This study is based on the metallographic observation of the surface state after immersion. Initially, physiological media (Ringer's Solution) with a chemical composition like body fluids were used. To accelerate the corrosion phenomenon, more aggressive media were used, such as nitric acid 2% (HNO_3) and sodium-chloric acid 3% (NaCl). After immersion in each medium, the analysis was performed using SEM observations to assess the surface state and any material degradation [34, 35].

EXPERIMENTAL MATERIALS AND TECHNIQUES

The alloy named AISI 316L according to the American standard is available in the form of 1 mm thick sheet. The samples used are cut into small sizes with approximate dimensions of 1×1 cm. Its chemical composition is presented in Table 3.

Potentiostatic and potentiodynamic tests are performed to evaluate and compare the currents, potentials and corrosion rates of the four samples

Table 3. Elemental composition of AISI 316L

Element	Fe	Cr	Ni	Mo	Mn	C	S	P	Si
Composition (% wt.)	60–65	17–19	13–15.5	2–3	2	<0.03	0.01	0.025	0.75

immersed in the prepared electrolytes. The samples are tested under the conditions similar to those used in vivo and in vitro. After the polarization tests, the variations in the surface morphology of each sample are recorded and captured using an optical microscope at the corrosion laboratory. Prior to testing, each sample matured using a standardized pretreatment; mechanical polishing with a series of silicon carbide abrasive papers to grit 1200, followed by ultrasonic cleaning in ethanol for ten minutes and rinsed with deionized water. This process was applied in order to remove contaminants, minimize residual stresses, and provide the same surface finish for all electrochemical investigations.

For all tests, a 200 ml electrolyte solution was used in electrochemical cells, ensuring the sample is covered by at least 15 mm. The electrolyte consists of Ringer's solution or saline. The immersion time of the sample in the reconstituted media and changes in body temperature were also considered. Different cases were analyzed, and several tests were conducted to evaluate the corrosion behavior of 316L SS. The experimental setup for plotting polarization curves is as follows: a thermostated bath ensuring the stability of the electrolyte temperature; a three-electrode electrochemical cell with a double wall allowing water circulation to maintain the reaction medium at a constant temperature of $T = 37\text{ }^{\circ}\text{C} \pm 0.4\text{ }^{\circ}\text{C}$; the electrolyte is renewed for each manipulation. After 2 hours of immersion (reaching the steady state), polarization curves are plotted for an over-voltage range of $[-400\text{ mV}, +400\text{ mV}]$.

For separate potentiodynamic polarization tests, the samples were immersed into the test electrolyte (i.e. Ringers solution, 3% – NaCl, or, 2% – HNO_3) for 2 hours to ensure that the sample reached a state of steady-state open circuit potential (OCP). Subsequently, the samples were polarized to produce polarization curves by scanning the potential from -400 mV to $+400\text{ mV}$ versus Ag/AgCl at a scan rate of 1 mV/s . The corrosion current density (i_{corr}) and the corrosion potential (E_{corr}) were obtained from Tafel extrapolation of the polarization curves. Polarization resistance (R_p) was calculated from the linear region, near

E_{corr} . Moreover, potentiostatic measurements were performed that hold the sample at a fixed potential (typically at the E_{corr} value) were taken, and the current density recorded over time, to examine the passivation behavior and passivation stability.

Knowing that i_{corr} is a qualitative indicator of the state of corrosion of a metal substrate in a known environment. E_{corr} is continuously recorded using the software which is linked to the potentiostat.

The evolution of the abandonment potential of the sample studied as a function of time, for an immersion period of one hour, makes it possible to follow the establishment of the steady state. These measurements also make it possible to reveal possible transitions from an active state to a passive state of the metal and vice versa. However, these tests do not provide the information on the corrosion kinetics. The potential scan starts at a voltage of -400 mV relative to the E_{corr} value and ends at a voltage of $+400\text{ mV}$ again relative to the E_{corr} value obtained during the OCP, the scan speed is set to 0.25 mV/s .

The determination of the i_{corr} and the E_{corr} is performed by extrapolating the anodic and cathodic Tafel lines to the corrosion potential E_{corr} . The point of intersection gives us directly $\log(i_{\text{corr}})$ from which i_{corr} and E_{corr} .

Thus, the determination of the corrosion rate and the polarization resistance from the Tafel curve is possible, the determination of the two parameters are explained in the following paragraphs. V_{corr} expressed in $(\text{mm} \cdot \text{year}^{-1})$, and is calculated by applying the following relation:

$$V_{\text{corr}} = i_{\text{corr}} \cdot t \cdot M \cdot 10/n \cdot F \cdot d \quad (1)$$

where: i_{corr} – the current density ($\text{A} \cdot \text{cm}^{-2}$), t – the time corresponding to one year, M – the average atomic mass of the alloy studied (g/mol), n – the valence and d – the density of the material (g/cm^3).

The inverse of the slope of the stationary polarization curve is the polarization resistance R_p , measured at the corrosion potential. The fastest way to obtain R_p is to impose small triangular variations ΔV around the corrosion potential, and to measure the resulting variations ΔI .

The accuracy of the results is low, because the I-E curves rarely obey Tafel's law, which is why most experimental devices are based on the determination of the polarization resistance R_p [11]. It is expressed as a function of the Tafel coefficients and the corrosion current:

$$R_p = \frac{b_a \cdot |b_c|}{2.3 \cdot (b_a + |b_c|)} \cdot i_{\text{corr}} \quad (2)$$

where: R_p – the polarization resistance ($\text{W} \cdot \text{cm}^2$),
 b_a – anodic Tafel slope (V), b_c – cathodic
 tafel slope (V), i_{corr} – (A/cm^2).

RESULTS AND DISCUSSION

Figure 1 shows the polarization curve $\log i = f(E)$ evolution of the current density as a function of the potential of a 316L steel in a Ringer's solution. The values of corrosion potential, corrosion current and corrosion speed are taken from the application of Tafel's law using the Versa-studio software and are grouped in Table 4.

From the results obtained in Ringer's solution (simulated in physiological medium), it was possible to conclude that the corrosion rate for 316L stainless steel in Ringer's solution is $3.52 \cdot 10^{-3} \text{ m} \cdot \text{year}^{-1}$, this rate is acceptable in the corrosion domain and shows a better behavior of 316L steel with respect to corrosion in a Ringer's solution. The passivation domain increases

proportionally to the immersion time as well as to the potential, this can be explained by the construction of a highly resistive passive film on the surface of the SS exposed to Ringer's solution. All the results obtained are relative to the measured electrochemical parameters and they are also perfectly correlatable between them.

Figure 2 shows the evolution of the logarithm of the current density as a function of the potential of 316L steel in a 3%NaCl solution. The values of corrosion potential, corrosion current and corrosion speed derived from the application of Tafel's law are grouped in Table 5.

From the results obtained in the 3% NaCl solution, it was possible to conclude that the shape of the curve that the Cl^- chlorides found in the solution attack the surface of the metal which increases the rate of pitting corrosion, so the potential becomes less noble and the corrosion current increases, which does not allow for good corrosion resistance.

Figure 3 shows the polarization curve $\log i = f(E)$ shows the evolution of the logarithm of the current density as a function of the potential of the 316L steel in the 2% HNO_3 solution. The values of corrosion potential, corrosion current and corrosion rate are taken from the application of Tafel's law using the Versa-studio software, and are grouped in Table 6.

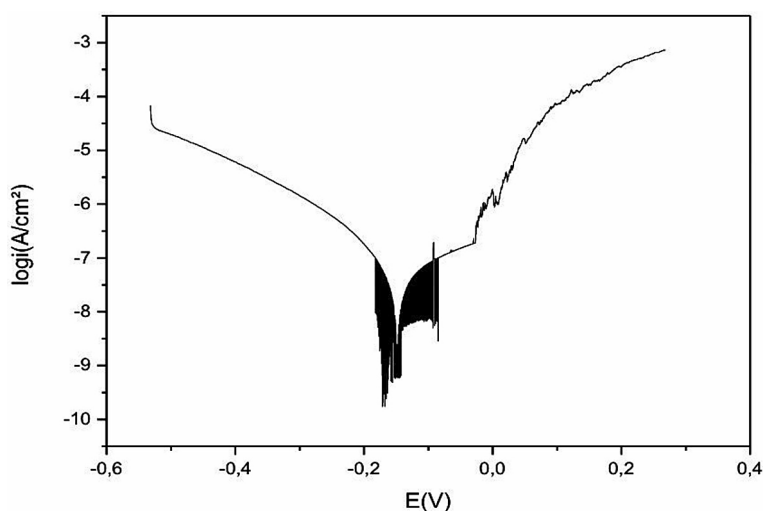


Figure 1. Potentiodynamic curve of type 316L SS in Ringer's solution

Table 4. Potentiodynamic results for 316L SS in Ringer's solution

Corrosion parameter	E_{corr} (mV)	i_{corr} (nA/cm ²)	V_{corr} (mm/year)
Values	-123.91	44.54	3.52×10^{-3}

Table 5. Potentiodynamic results for 316L stainless steel in 2% (HNO₃). Tafel slopes: The slopes of the linear regions of the anodic and cathodic branches of the polarization curve used to interpret the electrochemical kinetics.

Corrosion parameter	E _{corr} (mV)	i _{corr} (nA/cm ²)	V _{corr} (mm/year)
Values	-64.75	38.76	3.08

Table 6. Potentiodynamic results for 316L SS in 3%NaCl

Corrosion parameter	E _{corr} (mV)	i _{corr} (nA/cm ²)	V _{corr} (mm/year)
Values	-83.43	115.22	9.12 × 10 ⁻³

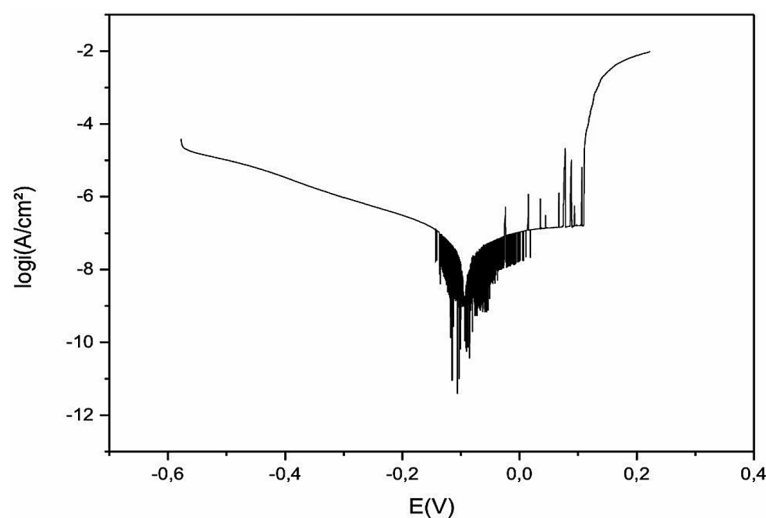


Figure 2. Potentiodynamic curve of type 316L SS in 3%NaCl solution

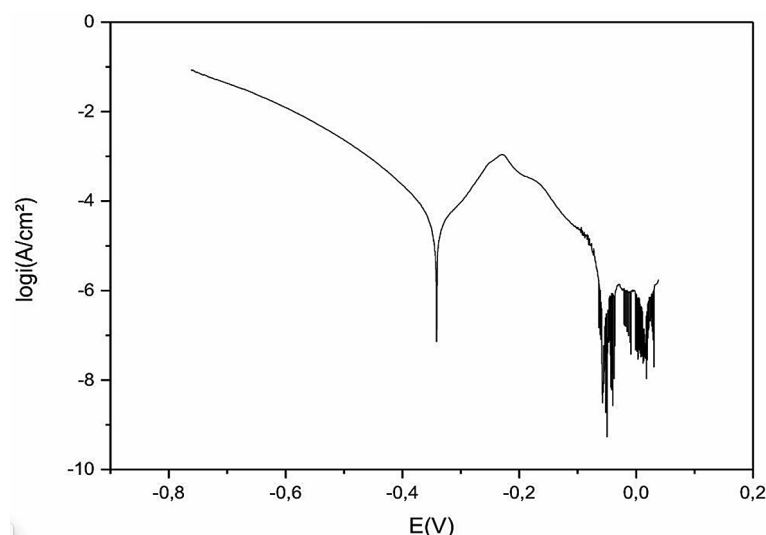


Figure 3. Potentiodynamic curve of type 316L SS in 2%(HNO₃) solution

From the results obtained in the 2% HNO₃ solution, it was possible to conclude that: The literature data [36, 37] reveal that the SS grades containing molybdenum as a minor element “grade 316L” are able to spontaneously form a passive

layer in a non-oxidizing acid. Other researchers [38, 39] reported that the existence of molybdenum in the stable passive film indicates its important role in determining the environmental behavior of SS in the HNO₃ environment, they found

that molybdenum, one of the noble elements of austenitic stainless alloy, exhibits improved passivation performance when exposed to a HNO_3 solution [40, 41].

The Tafel slopes b_c and b_a were determined directly from the Tafel lines, the values of these two relative parameters for each solution are grouped in Table 7. The results of the polarization resistance calculations are grouped in Table 8.

According to the results obtained in Table 7, Ringer's solution presents the highest values of polarization resistance followed by that of HNO_3 . The lowest value of the polarization resistance is that obtained for the 3%NaCl solution, this is due to the presence of chlorides which increase the corrosion rate and therefore decrease the polarization resistance.

From comparing the electrochemical parameters measured from all the polarization curves obtained in the different solutions of this study, it was noted that: Ringer's solution presents the best electrochemical quantities. The sample treated in an electrochemical cell containing a simulated solution of the physiological medium of the human body "Ringer's solution" presents the lowest

corrosion current density, and therefore it presents the lowest corrosion rate, this is due to the formation of a passive layer that protects the material and decreases the corrosion rate. Also, 316L SS in Ringer's solution presents the highest polarization resistance comparing with other solutions, and this is due to the formation of a passive layer that protects the material and decreases the corrosion rate.

These results provide some information on the interaction between 316L SS and acidic, neutral, chlorinated environments. The variation of the potential value with the immersion time can be explained by the electrochemical reaction that begins to take place between the medium and the exposed surface of the metallic substrate, more or

less adherent, causing a relative stability of the abandonment potential.

Stainless steels are passivable materials sensitive to pitting corrosion in the presence of specific aggressive species. These are most often the chloride ions Cl^- , which are the most aggressive and play an important role in the mechanism of initiation and development of pitting. Pitting corrosion is linked to very localized attacks of heterogeneities in the film and which result in local deterioration of the passive layer, thus exposing the metal on a very small surface area "anodic zone" compared to the areas remaining protected "cathodic zones". This process of deterioration of the material generally leads to a phenomenon of generalized corrosion for ordinary steels.

The stabilization of the passive film at higher chromium content in the conducted studies finds a direct correlate in the more recent findings from Archives of Metallurgy and Materials Engineering on the effect of alloy composition on surface passivation [42].

The inhibitive effect of carbonate ions on pitting corrosion finds support in recent electrochemical investigations published in JAMME that have scrutinized ion-specific corrosion behaviors [43].

The surface of the samples was further analyzed using SEM imaging technique. A very significant increase in the corrosion rate can be observed in the case of 3% NaCl and 2% HNO_3 solutions, which results in an increase in the size of the pits and the formation of other pits. The case of 316L steel has undergone considerable degradation, the pits are of a large size and cover a large surface. In the case of ringer solution, small pits appear, very far apart from each other (Figure 4a). In the case of immersion in NaCl solution, the first signs of larger corrosion were observed (Figure 4b). The only form of corrosion observed is pitting. The number and size of the

Table 7. Tafel slope values for each solution

Tafel slope (mV)	Ringer's solution	3% NaCl	2% HNO_3
Cathodic slope (b_c)	127.76	195.24	-431
Anodic slope (b_a)	83.76	1368	152

Table 8. Calculated values of polarization resistance for each solution

Solution	Ringer's Solution	3% NaCl	2% HNO_3
R_p ($\Omega \cdot \text{cm}^2$)	49.73×10^7	64.21×10^4	12.65×10^5

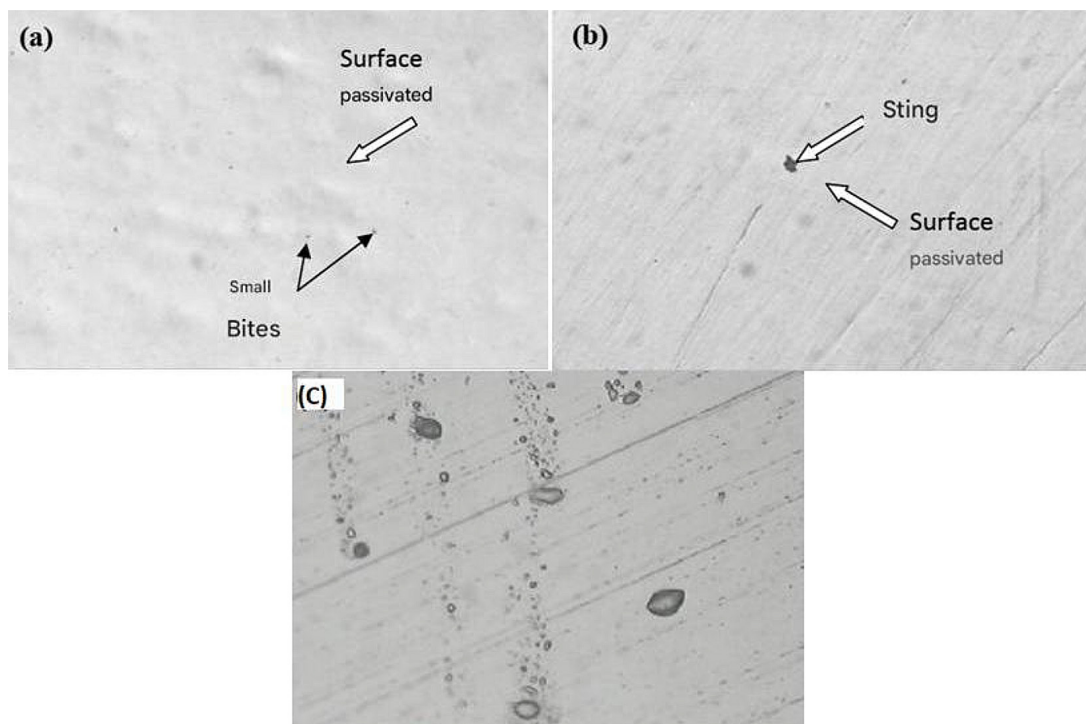


Figure 4. SEM images of Surface of samples after corrosion test in (a) Ringer's solution, (b) 3% NaCl solution and (c) 2% HNO_3 solution

pits increase as HNO_3 solution is used. As in the case of immersion in 2% nitric acid, the degradation (size and number of pits) of the 316L steel is the most significant at all times compared to the other solutions.

Quantitative analysis of the SEM micrographs revealed the pit diameters in sodium chloride solution were $2.1\text{--}8.7\text{ }\mu\text{m}$ (mean $4.3 \pm 1.2\text{ }\mu\text{m}$) and in Ringer's solution was $0.5\text{--}3.2\text{ }\mu\text{m}$ (mean $1.8 \pm 0.6\text{ }\mu\text{m}$), indicating more extensive localized corrosion was evident in the more aggressive saline media. Depth profiling through cross-section analysis on the SEM permitted the average figure of depth of pits compared to the surface width of the pits to be calculated, averaged 1:2.3 (surface width: subsurface propagation) whilst in chloride environments, and was consistent with the mechanisms of pitting studies in recent contemporary literature in the field of biomaterials research. The statistical distribution of pit diameters showed ca. 72% of pits were recorded below $5\text{ }\mu\text{m}$ diameter pits in Ringer's solution; however, descriptively only 38% were reported as $5\text{ }\mu\text{m}$ diameter in the sodium chloride solution, thus highlighting the inhibitory effect of carbonate ions influencing the propagation depth of pits better in a Ringer's solution. Quantifiable metrics provided in this paper present reproducible figures for clinicians

to compare the extent of corrosion for devices in different physiological simulations.

The Chromium atoms in steel react with oxygen in the air and form a protective layer of chromium oxide. Passivation or passivity represents a state of metals or alloys in which their corrosion rate is significantly reduced by the presence of a natural or artificial passive film, linked to what it would be in the absence of this film. In the case of 316L SS, this passive film appears spontaneously by oxidation, because the oxide formed on the surface is insoluble and constitutes an obstacle that slows down subsequent processes, in an aqueous medium, the formation of this film is linked to a range of electrochemical potential as well as a pH range in which the oxide is stable.

The corrosion processes of AISI 316L SS in different simulated physiological solutions are governed by the interplay between alloy chemistry, the passive film stability, and the specific ionic structure of the solution. In Ringer's solution, the presence of carbonate ions (CO_3^{2-}) retards pitting corrosion, perhaps due to the capacity of the carbonate ions to compete with the aggressive chloride ions (Cl^-) for adsorption sites on the protective film and stabilize the oxide protective layer. Conversely, in the NaCl solution, the heightened concentration of chloride ions causes

localized degradation of the passive film with resultant increased pitting and raised corrosion current densities in our electrochemical studies. The low carbon content in the 316L stainless steel further reduces the risk of intergranular corrosion by minimizing carbide precipitation at grain boundaries, hence maintaining the integrity of the passive film. These findings are consistent with the current literature that highlights the critical importance of alloying elements such as chromium and molybdenum to enhance passivation and delay localized corrosion in biomedical alloys. Besides, the observed differences in pit morphology and distribution between test media highlight the importance of both environmental chemistry and microstructural homogeneity in governing corrosion susceptibility. This general understanding of mechanisms of corrosion supports the selection and optimization of stainless steel alloys for biomedical use, as also emphasized in recent literature [44–47].

CONCLUSIONS

From this study, it has been found that 316L SS samples exhibit better corrosion behavior in Ringer's solution compared to other media studied. The electrochemical quantities taken from the tests confirm that our biomaterial is more resistant to corrosion in Ringer's solution. Moreover, this is reflected by a high polarization resistance with a low current density in the presence of this solution. The presence of carbonate ions in Ringer's solution acts as a pitting

The low carbon content in 316L SS prevents the formation of carbides in the grain boundaries, in particular chromium carbides Cr₂₃C₆, which are very stable compounds but do not prevent iron oxidation and promote intergranular corrosion of the biomaterial. Proper use of stainless steels therefore requires a metal of very high homogeneity to avoid local corrosion and a transition from the active state to the passive state at all points of the exposed surface. Several factors can influence the transport of ions through the protective film, such as: natural composition, structure, film thickness, and the existence of defects. Mainly, the nature and stability of a passive film of a particular metal or alloy will depend on environmental conditions, such as electrolyte composition, redox conditions, exposure, time and temperature. Increasing the chromium content

decreases the passivation current density and thus promotes the passivation of the steel. An increase in the pH value leads to a decrease in the passivation density of current.

These results have key implications for the selection and improvement of biomaterials for clinical use. The fact that 316L SS demonstrates increased corrosion resistance under physiologically relevant conditions supports its continued use in temporary and permanent orthopedic implants, dental tools, and surgical instruments where material integrity and biocompatibility are critical for longevity. Furthermore, identification of the influence of electrolyte composition on corrosion mechanisms has the potential to create more discriminating selection during the design of implantable devices, surface treatment, and alloy composition to optimize patient safety and clinical performance even further. Subsequent research will have to focus on in vivo testing and sophisticated surface engineering methods to optimize the corrosion resistance and lifespan of metallic biomaterials under complex biological conditions.

REFERENCES

1. Todros S, Todesco M, Bagno A. Biomaterials and their biomedical applications: From replacement to regeneration. *Processes*. 2021;9(11):1949. doi: 10.3390/pr9111949.
2. Al-Shalawi FD, Mohamed Ariff AH, Jung D-W, Mohd Ariffin MKA, Seng Kim CL, Brabazon D, et al. Biomaterials as implants in the orthopedic field for regenerative medicine: metal versus synthetic polymers. *Polymers*. 2023;15(12):2601. doi: 10.3390/polym15122601
3. Bazaka O, Bazaka K, Kingshott P, Crawford RJ, Ivanova EP. Metallic Implants for Biomedical Applications. In: Spicer C, editor. *The Chemistry of Inorganic Biomaterials*: Royal Society of Chemistry; 2021;1–98.
4. Davis R, Singh A, Jackson MJ, Coelho RT, Prakash D, Charalambous CP, et al. A comprehensive review on metallic implant biomaterials and their subtractive manufacturing. *The International journal, advanced manufacturing technology*. 2022;120(3–4):1473–530. doi: 10.1007/s00170-022-08770-8.
5. Moghadasi K, Mohd Isa MS, Ariffin MA, Mohd jamil MZ, Raja S, Wu B, et al. A review on biomedical implant materials and the effect of friction stir based techniques on their mechanical and tribological properties. *Journal of Materials Research*

- and Technology. 2022;17:1054-121. doi: <https://doi.org/10.1016/j.jmrt.2022.01.050>.
6. Knetsch MLW. Evolution of Current and Future Concepts of Biocompatibility Testing. In: Dumitriu S, Popa V, editors. *Polymeric Biomaterials*: CRC Press; 2013;377–414.
7. Baltatu M-S, Burduhos-Nergis D-D, Burduhos-Nergis DP, Vizureanu P. *Advanced metallic biomaterials: Materials Research Foundations*; 2022.
8. Mitra M, Mitra S, Nandi DK. Human Physiology and Metabolism: An Overview. In: Mitra M, Mitra S, Nandi DK, editors. *Body Recomposition*: CRC Press; 2024;43–58.
9. Iswanto PT, Faqihudin A, Sadida HM, editors. *Distribution of Hardness, Surface Roughness and Wettability of AISI 316L Induced by Shot Peening with Different Duration and Shooting Distance* 2020: IOP Publishing.
10. Kostova I. The role of complexes of biogenic metals in living organisms. *Inorganics*. 2023;11(2):56. doi: 10.3390/inorganics11020056.
11. Jastrzab R, Lomozik L, Tylkowski B. Complexes of biogenic amines in their role in living systems. *Physical Sciences Reviews*. 2016;1(6). doi: 10.1515/psr-2016-0003.
12. Liu P, Hu L, Zhao X, Zhang Q, Yu Z, Hu J, et al. Investigation of microstructure and corrosion behavior of weathering steel in aqueous solution containing different anions for simulating service environments. *Corrosion Science*. 2020;170:108686. doi: 10.1016/j.corsci.2020.108686.
13. Guo Y, Xue J, Zhang J, Chen Q, Fan L, Tang C, et al. Effect of corrosion products on the inhibitory performance of imidazolium ionic liquid toward carbon steel in CO₂-saturated NaCl brine. *Colloids and Surfaces A: Physicochemical and Engineering Aspects*. 2022;651:129135. doi: 10.1016/j.colsurfa.2022.129135.
14. Armiento AR, Hatt LP, Sanchez Rosenberg G, Thompson K, Stoddart MJ. Functional biomaterials for bone regeneration: a lesson in complex biology. *Advanced Functional Materials*. 2020;30(44):1909874. doi: 10.1002/adfm.201909874.
15. Souza JCM, Apaza-Bedoya K, Benfatti CAM, Silva FS, Henriques B. A comprehensive review on the corrosion pathways of titanium dental implants and their biological adverse effects. *Metals*. 2020;10(9):1272. doi: 10.3390/met10091272.
16. Nagay BE, Cordeiro JM, Barao VAR. Insight into corrosion of dental implants: from biochemical mechanisms to designing corrosion-resistant materials. *Current oral health reports*. 2022;9(2):7–21. doi: 10.1007/s40496-022-00306-z.
17. Pilliar RM. *Metallic biomaterials*. In: Narayan R, editor. *Biomedical materials*. Boston, MA: Springer; 2021;41–81.
18. Thanigaivel S, Priya AK, Balakrishnan D, Dutta K, Rajendran S, Soto-Moscoso M. Insight on recent development in metallic biomaterials: Strategies involving synthesis, types and surface modification for advanced therapeutic and biomedical applications. *Biochemical Engineering Journal*. 2022;187:108522. doi: 10.1016/j.bej.2022.108522.
19. Mani G, Porter D, Collins S, Schatz T, Ornberg A, Shulfer R. A review on manufacturing processes of cobalt-chromium alloy implants and its impact on corrosion resistance and biocompatibility. *Journal of Biomedical Materials Research Part B: Applied Biomaterials*. 2024;112(6):e35431. doi: 10.1002/jbm.b.35431.
20. Wu W, Luo J, Li D, Feng X, Tang L, Fang Z, et al. Experimental investigation of heat transfer performance of a finned-tube heat exchanger under frosting conditions. *Sustainable Cities and Society*. 2022;80:103752. doi: 10.1016/j.scs.2022.103752.
21. Pandey A, Awasthi A, Saxena KK. Metallic implants with properties and latest production techniques: a review. *Advances in Materials and Processing Technologies*. 2020;6(2):405–40. doi: 10.1080/2374068X.2020.1731236.
22. Smith P. 8 - Glossaries and Abbreviations. In: Smith P, editor. *Piping Materials Guide*. Burlington: Gulf Professional Publishing; 2005;243–332.
23. Snizhnoi G. Dependence of corrosion resistance of austenitic chromium-nickel steels on the magnetic state of austenite. In: Ambrish S, editor. *Stainless Steels*. Rijeka: IntechOpen; 2022;4.
24. Snizhnoi GV, Snizhnoi VL. Magnetometric assessment of the influence of chemical elements on the corrosion of austenitic Fe-Cr-Ni alloys. *Materials Science*. 2024. doi: 10.1007/s11003-024-00857-9.
25. Etefagh AH, Guo S, Raush J. Corrosion performance of additively manufactured stainless steel parts: A review. *Additive manufacturing*. 2021;37:101689. doi: 10.1016/j.addma.2020.101689.
26. Kaae PH, Eikeland EZ. Corrosion Performance of Additively Manufactured Stainless Steel by Binder Jetting. *IOP Conference Series: Materials Science and Engineering*. 2022;1249(1):012051. doi: 10.1088/1757-899X/1249/1/012051.
27. Ghaidan AAA, Jomah AJS. Enhancing mechanical properties of low alloy steel through novel molten Bi-Ga austempering. *Diyala Journal of Engineering Sciences*. 2024;173–81.
28. Shehab AA, Nawi SA, Al-Rubaiy A, Hammoudi Z, Hafedh SA, Abass MH, et al. CO₂ laser spot welding of thin sheets AISI 321 austenitic stainless steel. *Archives of Materials Science and Engineering*. 2020;106(2).
29. Mohamed MT, Nawi SA, Algailani HM, Al-rubaiy AAAG, Mahmoud AK, Farman S, et al. Evaluation of the mechanical performance of

- iron–polymethyl methacrylate and polystyrene polymer products based on alumina nanomaterials. *Advances in Science and Technology Research Journal*. 2025;19(3):202–10.
30. Nawi SA, Mohammed HB, Jasim AN, Sharaf HK, Muhammad MT. Numerical analysis of the influence of the rolling speed on the cold rolling under specific thermal condition of the AA 5052-O aluminum alloy. *Journal of Advanced Research in Fluid Mechanics and Thermal Sciences*. 2024;122(1):69–79.
31. Alrubaiy AAAG, Aljuhashy RM, Al-Bakri BAR. Experimental investigation of diesel-WCOB engine performance with a small proportion of ethanol/isobutanol as a fuel additive. *International Journal of Integrated Engineering*. 2023;15(7):82–8.
32. Pathote D, Jaiswal D, Singh V, Behera CK. Optimization of electrochemical corrosion behavior of 316L stainless steel as an effective biomaterial for orthopedic applications. *Materials today: proceedings*. 2022;57:265–9. doi: 10.1016/j.matpr.2022.02.501.
33. Zatkaličová V, Uhrčík M, Markovičová L, Pastierovičová L, Kuchariková L. The effect of sensitization on the susceptibility of AISI 316L biomaterial to pitting corrosion. *Materials*. 2023;16(16):5714. doi: 10.3390/ma16165714.
34. Morsiya C. A review on parameters affecting properties of biomaterial SS 316L. *Australian Journal of Mechanical Engineering*. 2022;20(3):803–13. doi: 10.1080/14484846.2020.1752975.
35. Benčina M, Kovač J, Lakota K, Žigon P, Kralj-Iglič V, Iglič A, et al. Chapter Three - Advancements and biocompatibility of stainless steel: Improved cell membrane adhesion and antibacterial properties. In: Iglič A, Rappolt M, Losada-Pérez P, editors. *Advances in Biomembranes and Lipid Self-Assembly*. 40: Academic Press; 2024;33–53.
36. Hryniewicz T, Rokosz K, Rokicki R. Electrochemical and XPS studies of AISI 316L stainless steel after electropolishing in a magnetic field. *Corrosion Science*. 2008;50:2676–81. doi: 10.1016/j.corsci.2008.06.048.
37. Lai WY, Zhao WZ, Yin ZF, Zhang J. Electrochemical and XPS studies on corrosion behaviours of AISI 304 and AISI 316 stainless steels under plastic deformation in sulphuric acid solution. *Surface and Interface Analysis*. 2012;44(5):505–12. doi: https://doi.org/10.1002/sia.3830.
38. Håkansson E. Inhibition of pitting corrosion in 316L stainless steel: an evaluation of the phenomena and method to facilitate material selection for processing equipment: Lund University; 2024.
39. Voisin T, Shi R, Zhu Y, Qi Z, Wu M, Sen-Britain S, et al. Pitting corrosion in 316L stainless steel fabricated by laser powder bed fusion additive manufacturing: a review and perspective. *JOM*. 2022;74(4):1668–89. doi: 10.1007/s11837-022-05206-2.
40. Tan L, Wang Z, Ma Y. Tribocorrosion behavior and degradation mechanism of 316L stainless steel in typical corrosive media. *Acta Metallurgica Sinica (English Letters)*. 2021;34:813–24. doi: 10.1007/s40195-020-01182-1.
41. Liu Y, Liu L, Li S, Wang R, Guo P, Wang A, et al. Accelerated deterioration mechanism of 316L stainless steel in NaCl solution under the intermittent tribocorrosion process. *Journal of Materials Science & Technology*. 2022;121:67–79. doi: https://doi.org/10.1016/j.jmst.2022.01.011.
42. Iswanto PT, Akhyar H, Faqihudin A. Effect of shot peening on microstructure, hardness, and corrosion resistance of AISI 316L. *Journal of Achievements in materials and manufacturing Engineering*. 2018;89(1):19–26.
43. Prabakaran K, Rajeswari S. Electrochemical, SEM and XPS investigations on phosphoric acid treated surgical grade type 316L SS for biomedical applications. *Journal of applied electrochemistry*. 2009;39:887–97.
44. Bocchetta P, Chen L-Y, Tardelli JDC, Reis ACd, Almeraya-Calderón F, Leo P. Passive layers and corrosion resistance of biomedical Ti-6Al-4V and β -Ti alloys. *Coatings*. 2021;11(5):487.
45. Man C, Dong C, Liu T, Kong D, Wang D, Li X. The enhancement of microstructure on the passive and pitting behaviors of selective laser melting 316L SS in simulated body fluid. *Applied Surface Science*. 2019;467:193–205.
46. Bahrawy A, El-Rabiei M, Elfiky H, Elsayed N, Arafa M, Negem M. Electrochemical behaviour of some commercial stainless steel alloys in simulated body fluid electrolytes. *Anti-Corrosion Methods and Materials*. 2021;68(3):167–81.
47. Bidhendi HRA, Pouranvari M. Corrosion study of metallic biomaterials in simulated body fluid. *Metallurgical and Materials Engineering*. 2012.